



COLLEGE OF ENGINEERING
THE UNIVERSITY OF TOLEDO



Magnetic Sensor for Nondestructive Evaluation of Deteriorated Prestressing Strand – Phase II

**August 2011
Final Report**

Principal Investigator:

Douglas K. Nims, Ph.D., P.E.
Associate Professor, Civil Engineering
The University of Toledo

Co-PI:

Vijay Devabhaktuni, Ph.D., P.Eng. (Alberta)
Associate Professor, Electrical Engineering and Computer Science
The University of Toledo

Prepared for
The University of Toledo University Transportation Center
Research and Tech Complex - R1
2801 W. Bancroft, Mail Stop 218
Toledo, OH 43606-3390

DISCLAIMER

The contents of this report reflect the views of the authors, who are responsible for the facts and the accuracy of the information presented herein. This document is disseminated under the sponsorship of the Department of Transportation University Transportation Centers Program, in the interest of information exchange. The U.S. Government assumes no liability for the contents or use thereof.

Abstract

This report gives an account of the execution and achievements in Phase II of the project completed through August 2011. The main objective of this project is to advance the practical development of a nondestructive testing and evaluation method using the magnetic field technique to estimate corrosion in prestressing strands. The importance of developing such a method has been well established. Phase I and the literature review established the proof of concept for a magnetic inspection method. The magnetic technique of induced magnet field (IMF) was developed.

The overall goal of this project is to investigate the feasibility of a magnetic sensor to detect in-situ corrosion of prestressing strand in prestressed concrete bridge beams. Corrosion is a slow developing phenomenon which is not adequately detected using sensors currently in service. Despite national studies, no effective nondestructive sensor technology has been identified for prestressing strand corrosion. An effective sensor for corrosion will be able to get a snapshot of the corrosion in time by sensing the corrosion by-products or a direct change in member properties due to corrosion. This is a departure from the typical procedure of measuring a quantity, such as strain, which is a secondary effect of corrosion. The need for the proposed sensor is particularly acute in Ohio where there are many prestressed box girder bridges.

In phase II,

1. A magnet specifically designed for detecting corrosion in prestressing strand was designed, fabricated and procured.
2. The magnet was tested in the laboratory on bar, non-corroded strand and corroded strand. The ability to establish effective cross sectional area was established.
3. Funding was secured from an outside agency and the magnet was tested in the field.
4. In the field test, both the IMF and magnetic flux leakage techniques were used. Dissection showed both techniques were able to identify corrosion in a manner that could be used in bridge load rating. The researchers have also been working on developing a computer prediction model which uses measured IMF values from field tests to estimate cross sectional area of prestressing strands.
5. Developing a computer prediction model which uses measured IMF values from field tests to estimate cross sectional area of prestressing strands has begun.
6. An overview of the state of the art has been completed and the steps necessary to advance have been identified.

In Phase II, a larger yoke-shaped electromagnet was designed and fabricated that could provide a higher level of magnetic saturation for prestressing strands embedded in concrete and also allow an adequate signature of the remaining strand cross section. The research team has been successful in developing a commercial partnership with a large industrial electromagnet firm, Ohio Magnetics, Inc. The yoke-shaped electromagnet magnetizes the steel specimen from one

side along its length. The induced magnetic field in the steel gives a direct measure of the cross sectional area of the specimen. Laboratory experiments were conducted using AISI 1018 steel rods and AISI 1020 prestressing strands of different diameters. This was done using air-gaps and concrete blocks of different sizes between the electromagnet pole face and the specimen. The results showed that the magnetic field induced in the steel specimens was directly related to their cross sectional area. Tests were also performed for corroded specimens obtained from a demolished bridge. From the measured IMF values, the remaining cross sectional area of the strand was estimated. The actual cross section of the strand was measured by cutting the strand and removing the rust. A close match was found between measured and estimated values of cross section.

With these findings the researchers felt confident enough to test an adjacent box beam bridge that was scheduled for demolition. The field test was done as part of another project in the same duration of this project. They have thus been able to advance this IMF method to a stage where theoretical ability has been proven. Certain issues such as weight of equipment, temperature rise drift and knowing the distance between the strand and the electromagnet pole face accurately need to be addressed. It is felt that these issues can be solved in time which will bring this method close to practical realization.

Keywords

Concrete bridge, corrosion, deterioration, flaw detection, inspection equipment, magnetic, maintenance, prestressed concrete, reinforcing steel

Subject Categories

Maintenance, Bridges, Structures, Highways, Materials.

Contents

Abstract	iii
1. Introduction	1
2. The Problem Addressed in the Project	1
3. Project Approach	2
4. Literature Review	2
5. Design of the Electromagnet-Based Sensor	3
5.1 The Induced Magnetic Field (IMF) Concept	3
5.2 Design of Electromagnet	4
5.3 Sensors and Other Equipment	8
5.3.1 Hall Sensors	8
5.3.2 Data Acquisition and Recording	8
6. The Experiments with Yoke-Shaped Electromagnet Sensor	9
6.1 Experiments with AISI 1018 Cold-rolled Steel Bars	9
6.2 Experiments with Prestressing Strand	12
6.3 Experiments with Corroded Prestressing Strand	13
7. Results and Data Interpretation	14
7.1 Comparison of Steel Samples Magnetized in Air Gaps	14
7.2 Comparison of Steel Samples Magnetized in Concrete Blocks	15
7.3 Analysis for Corroded Prestressing Strand	16
8. Overview of Development of the IMF Sensor System	19
8.1 Field Test on Washington Waterloo Road Bridge	19
8.2 Present State-of-the-Art and Progress	20
9. Conclusions and Future Work	21
9.1 Conclusion	22
9.2 Future work	22
References	23
Appendix	25
Bipolar Electromagnet 16 in. x 6 in. Drawing	25

1. Introduction

The overall objective of this project is to develop a prototype sensor based on the induced magnetic field (IMF) method that can reliably estimate the remaining cross sectional area of exposed or hidden corroded prestressing strands in a laboratory setting. After advancing the understanding of the concepts of magnetization and obtaining a proof-of-concept for steel rods of small diameters (0.2 in) in Phase I, further development was carried out by designing, fabricating and using a research electromagnet-sensor in Phase II. This was tested in a laboratory using prestressing strands and steel rods of different diameters. Corroded prestressing strands were tested and their cross sectional area was estimated. The various technical details of this progress along with the suggestions for improvement of the technology for its practical realization have been detailed in this report. Field testing was also undertaken as part of an Ohio Department of Transportation project in collaboration with Dr. Al Ghorbanpoor, an expert in the magnetic flux leakage (MFL) method. Issues preventing practical implementation of the IMF method have also been identified.

2. The Problem Addressed in the Project

The goal of this project has been to develop an electromagnet which will act as a sensor to determine the remaining effective cross sectional area in corroded prestressing strand in concrete bridges. An accurate and convenient nondestructive inspection technique for detecting in-situ corrosion of prestressing strand, particularly in box beam bridges, will improve safety for the traveling public and assist in better maintenance planning. There is a population of existing box beam bridges and one in six new bridges built on public roads are adjacent box beams so there is present and future need for effective determination of corrosion of prestressing strand.

Visual inspection is the method currently used to detect corrosion in prestressing strands in box beam bridges. Visual inspection is not adequate even when it is known a priori that the structure has extensive deteriorated strand (Abi Shdid 2006, Scott 2006, Ferroni 2007, ODOT 2008).

Unexpected failure of prestressed concrete box beam bridges due to prestressing strand corrosion has occurred. To determine the remaining flexural capacity of a prestressed bridge, the engineer must know the remaining cross sectional area of the strand. The corrosion of the exposed strands is manifest, but their effective area must be estimated. The state of the strands where there is no spalling is unknown. It is desirable to be able to estimate the area of these strands without removing their cover. National studies have identified the development of an effective nondestructive sensor technology (FHWA 2010) as a research priority. Approximately 10% of the square footage of Ohio's bridges is box-girders, susceptible to prestressing strand corrosion (ODOT 2008).

In Phase I of the project it was shown that an electromagnet can be used to magnetize a steel bar from one side and give a measure of the effective cross sectional area of the bar from the induced magnetic field measurement. This magnetic field also depends on the distance of the electromagnet from the bar. However, the DC electromagnet used was insufficient to induce a magnetic field near a point of saturation in the specimen. Thus, the need to design and fabricate a stronger electromagnet which could be used for laboratory testing of the concept was proposed in

Phase II. Experiments are conducted to develop a relationship between the magnetic field induced in the steel strands and their cross sectional area. By doing this, a direct measure of the remaining cross section of prestressing stands can be obtained from measured magnetic field values. The main idea behind doing this is to know whether the electromagnet-sensor can be a useful tool to test a box beam bridge.

3. Project Approach

This project is a step on the road to the development of a practical sensor for in situ estimation of the cross sectional area of corroded prestressing strands. Development of a magnetic sensor would be a fundamental breakthrough and there would be follow-up research on implementation. The sensor, which is being developed, has the potential to spawn a product line and revolutionize inspection.

After the experiences from Phase I with the studies involving the parallel pole DC electromagnet, the next approach was to design and fabricate a yoke-shaped DC electromagnet-sensor. This sensor would be used to obtain a stronger proof-of concept and to determine if it can be used to perform practical field tests. The following approach was followed to bring about the final goals of this project:

- Design a prototype sensor based on magnetic principles and determine if it is promising enough to merit further development. Fabricate the electromagnet by engaging a commercial electromagnet manufacturer.
- Develop and execute a testing protocol to verify the sensor's ability to detect the cross sectional area of corroded prestressing strand in the laboratory. Perform experiments examining the effect of gaps between the magnet and the specimen. This will culminate in the measurement of specimens embedded in concrete.
- Perform tests on corroded strand specimens to estimate cross sectional area and compare to measured values of cross section.
- Seek external funding to further the sensor development.

4. Literature Review

The experiments conducted in Phase I of the project concluded that the induced magnetic field method has the capability to determine the cross sectional area of a steel rod or bar. The next step in the literature review was to look for existing ideas and designs of electromagnets used to magnetize elongated bodies of steel. Such examples were available in research papers regarding magnetic field testing of steel ropes or cables. Magnetic techniques have shown potential to identify various corrosion levels related to loss of section or fractures in prestressing strands (Jones *et al.* 2010; Naito and Jones 2010).

The remnant magnetic field method as proposed by Hillemeir and Scheel (1997, 1998), who developed a sensor where prestressing tendons are magnetized with a yoke-shaped electromagnet with up to 12 in. (300 mm) of concrete cover. They were successful in detecting fractures in prestressing wires. From this work it was perceived that the magnetic field induced in a ferromagnetic material is directly proportional to the cross sectional area of the specimen. The

team's aim, as stated earlier, is to determine the remaining cross sectional area along the length of a corroded prestressing strand. Knowing the current state of corrosion is necessary to estimating the capacity of the bridge. The current capacity at any time is expressed as a load rating (AASHTO 2011). Corrosion detection is important since fractures are developed as a consequence of corrosion. In Scheel's Ph.D. dissertation (Scheel 1997), the basic concept of the remnant magnetic method is described. He has also shown through experiments using a yoke-shaped electromagnet that the magnetization of steel strands through concrete is possible. However, it is used to detect fractures.

Rumiche, *et al.*, 2008, used a solenoid electromagnet which was toroid-like in shape, to achieve magnetic saturation of specimens. These experiments showed a linear relationship between the normalized mass loss and the magnetic saturation for all the sample specimens. However, the toroid cannot be used in a field application on a prestressed or post-tensioned beam.

The MFL method was introduced by Kusenberger (Kusenberger and Barton 1981) for investigations of the steel in prestressed concrete members. This method has been used on site for more than a decade to inspect prestressed tendons. In every case, measured corrosion or rupture signals have been confirmed to originate from "tendon corrosion or cracks" by visual inspection after opening the concrete (Ghorbanpoor *et al.* 2000).

Inputs from Dr. Gottfried Sawade at the University of Stuttgart, Germany were considered to design the magnetic field strength for the new electromagnet design. He is one of the researchers who have designed an electromagnet to detect fractures in prestressing steel (Sawade 2007).

5. Design of the Electromagnet-Based Sensor

This section describes the design of the yoke-shaped electromagnet based sensor and design parameters taken into consideration. It also explains the induced magnetic field concept which is the principle of measurement of this electromagnet-sensor. This prototype sensor was used to conduct experiments on prestressing strands and steel bars in determining the amount of mass loss due to corrosion. This prototype electromagnet is designed to produce stronger magnetization of the prestressing strands embedded up to 2 in. in depth. From experiments described in Phase I of the project, it was shown that the magnetization of the specimen to a level near magnetic saturation was not achieved using a parallel-pole electromagnet.

5.1 The Induced Magnetic Field (IMF) Concept

Consider the yoke-shaped electromagnet of Figure 1. The steel rod is placed between the poles of the electromagnet. Hall sensors are located at the pole faces to measure magnetic field induced in the specimen, during magnetization. Theoretically, a measurement taken under external magnetization gives the induced magnetic field in the magnetic circuit at a point of interest on the strand. The magnitude of the induced magnetic field depends on the cross sectional area of the steel strand at the measurement point above the Hall sensor. Figure 1 shows comparison of two steel rods of different diameters d_1 and d_2 under magnetization ($d_1 > d_2$). Magnetic field B_1 induced in the rod of diameter d_1 is higher than that of diameter d_2 . The electromagnet is yoke-shaped, which reduces the reluctance in the magnetic circuit, thus completing the flux path.

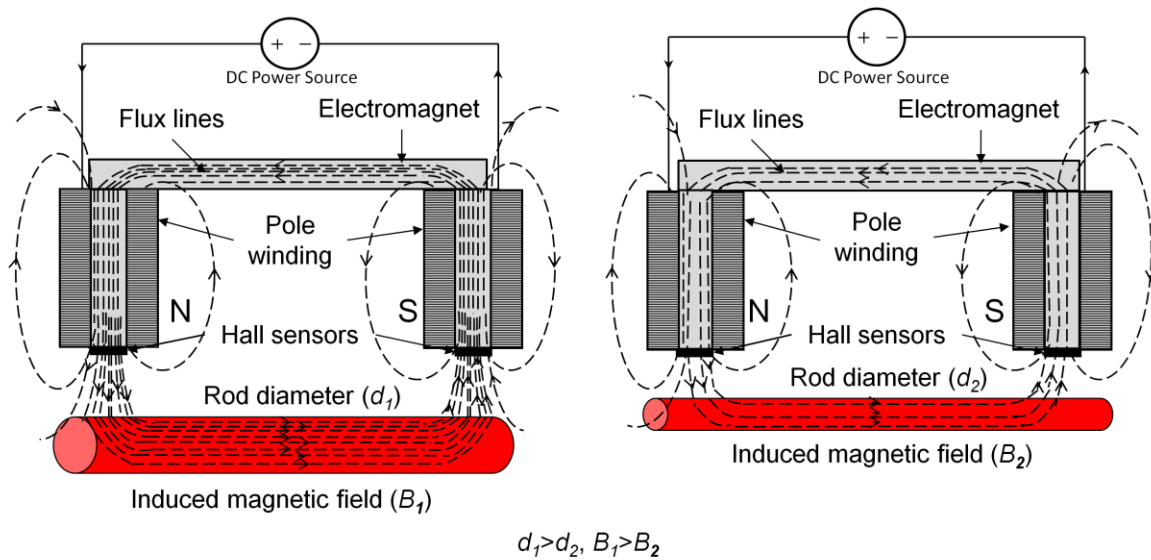


Figure 1. Illustration of induced magnetic fields in steel specimens of diameters d_1 and d_2 using a yoke-shaped electromagnet.

The magnetic field induced in the steel rod varies with the characteristics of the rod itself, such as cross sectional area, since the diameter of the rod is uniform. As such, the present condition of the rod can be determined through examination of the induced magnetic field strength. A comparison of the magnetic field strength of a non-corroded rod with that of a corroded rod can be used to estimate the remaining cross section of the corroded rod. The typical relationship between magnetic field and corrosion area can be explained as follows. Corrosion can be inferred as a change in cross sectional area. The change in magnetic induction with the change in effective cross sectional area of steel due to corrosion can be correlated to estimate corrosion in terms of mass loss of steel. A non-corroded specimen has a higher effective remaining cross sectional area compared to a corroded specimen with the same original diameter. In other words, a non-corroded rod would be induced with a magnetic field higher in magnitude than a corroded one. The magnetized rod will have a magnetic field depending on the sound steel under magnetization at any given time. The “induced magnetic field” in the rod will be measured using a “Hall effect” sensor located on the pole face of the electromagnet. The induced magnetic field in a corroded strand relative to that in a non-corroded sample with the same original diameter can potentially offer an estimate of the mass loss due to corrosion (or reduction in cross sectional area).

5.2 Design of Electromagnet

The yoke-shaped electromagnet shown in Figure 2 is seen as a suitable shape in order to have flux lines flow through the length of the steel rod. The maximum flux flow path is seen as dotted lines passing through the volume of the steel in contact with the pole faces.

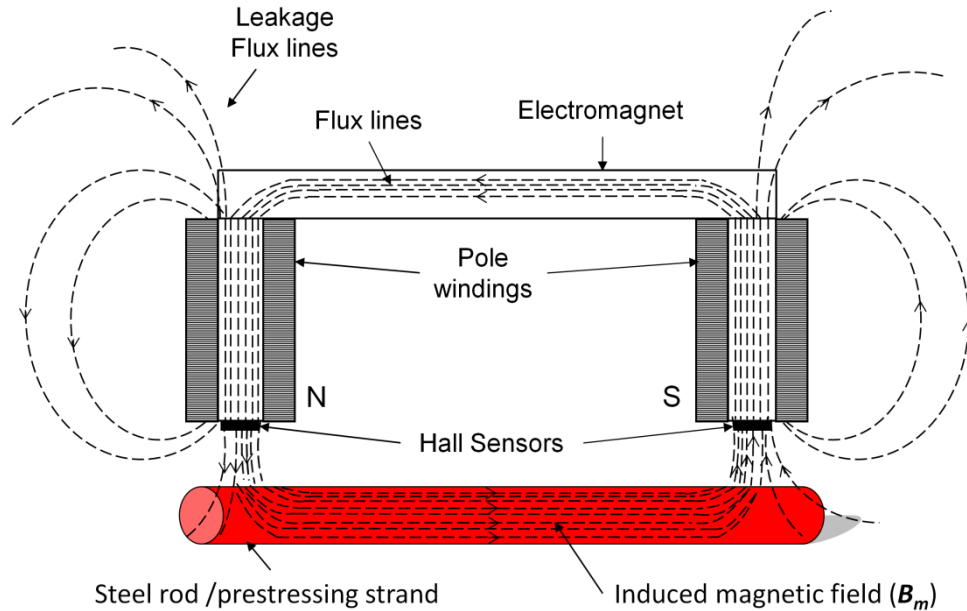


Figure 2. Flux lines through the steel specimen for a yoke shaped electromagnet.

In order that the steel rod achieves a level of near to complete magnetic saturation on its hysteresis loop, it is necessary that the magnetic lines of flux flow through the entire length of the rod during magnetization. Therefore, the design of the magnet should be such that it magnetizes maximum volume of the rod. According to the geometry of the rod, since it is long, maximum magnetization would occur when magnetic lines of flux flow along the length of the rod. When this happens the magnetic dipoles will align easily in north-south pole direction along the length of the rod. Aligning the dipoles along the length is much easier than having it transverse to the length of the rod. This will ensure that the magnitude of the induced magnetic field is sufficient enough to be a substantial measure of the cross sectional area of the prestressing strand.

The magnitude of the magnetic field generated by the electromagnet is also crucial and is designed to ensure that the specimen achieves a level near to magnetic saturation. In a field scenario to take measurements, the electromagnet will be moved along the length of the bridge magnetizing the strand inside it while taking measurements. In the laboratory however, steel rod or strand specimens would be placed above the pole faces and then magnetized to record measurements.

Measurements are taken by Hall sensors located on each of the pole faces. They measure the axial component of the induced magnetic field in the part of the steel rod/strand at the pole face. The rod/strand in contact with both ends of the yoke at the poles will complete the magnetic circuit. The important parameters for design of the electromagnet are thickness of rod/strand to be measured, permeability of the prestressing steel, and thickness of air gap or concrete cover as the case may be. For design considerations, the magnetic permeability of concrete was considered to have negligible effect on the magnetization. Later, experiments have been done to see the effects of concrete by comparing it to that done with air gaps.

One way of ensuring the magnitude of flux generated by the electromagnet is high is by having maximum flux lines flowing through the rod/strand using the path of least reluctance, described earlier. The magnitude of induced magnetic flux is also controlled by designing the Ampere-turns of the electromagnet. Thus, by having optimum Ampere-turns for the coil of the electromagnet the yoke can be operated in the region of magnetic saturation of its hysteresis loop.

The final design of the bipolar electromagnet has a current rating of 5 ADC. Dr. Sawade has also shared a sketch of the basic dimensions of his electromagnet design (see Figure 3). The value for magnetic field H suggested by him for the electromagnet was 150-200 A/cm at the pole face. The designed value for the electromagnet is 194 A/cm.

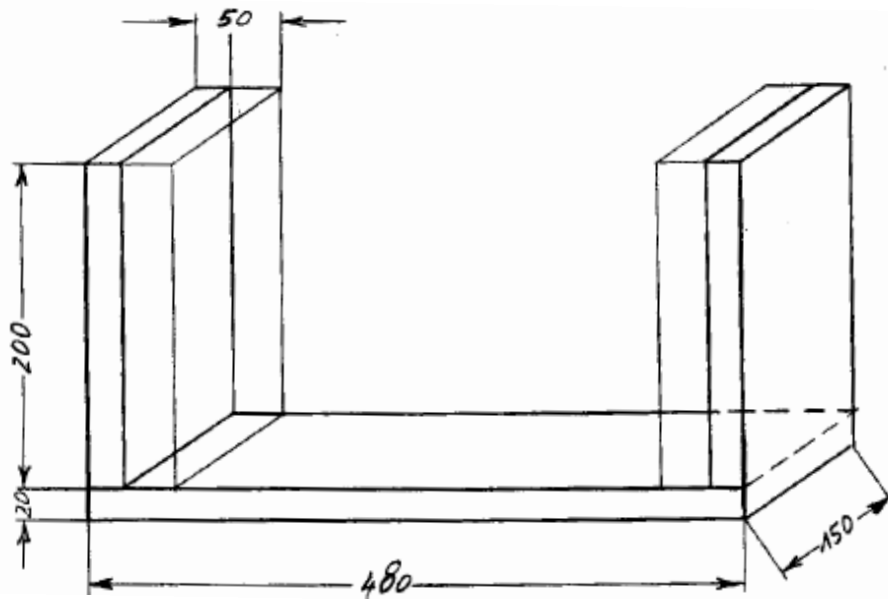


Figure 3: Sketch of electromagnet dimensions used by German researcher Dr. Gottfried Sawade, at University of Stuttgart, Germany, based on the one that he uses for detection of fractures in prestressing strand.

From preliminary experiments, it was seen that a value of around 200 A/cm would be suitable to saturate a prestressing strand about 0.5 in. diameter. The final dimensions of the fabricated electromagnet are 16 in. long, 6 in. wide and 7 in. high poles. The magnet is DC operated with a built-in rectifier, has a maximum power consumption of 0.56 kW and weighs approximately 235 lb. The electromagnet can be operated continuously for about 20 min.

A simulation plot of magnetic field generated by the electromagnet is shown in Figure 4. From the figure it can be seen that the open circuit magnetic field generated at the pole face is in the range of 0.13 T to 0.14 T. Figure 5 shows a graphical flux density plot for the electromagnet at various distances around its poles using the *Finite Element Method Magnetics* (FEMM) simulation tool. This electromagnet has a magnetic field strength of 0.135 T at the pole face and 0.087 T at $1\frac{3}{4}$ in. from the pole face. This final designed electromagnet was manufactured by

Ohio Magnetics (see Figure 6). An AutoCAD outline drawing of the same is available in Appendix A.

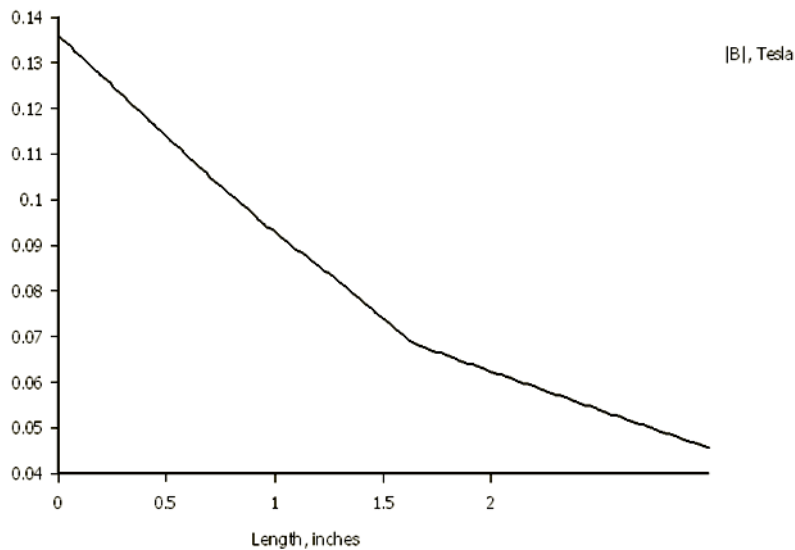


Figure 4: Magnetic flux density, $|B|$ [T] for various distances from the pole face of the 16 in. x 6 in. bipolar electromagnet using FEMM.

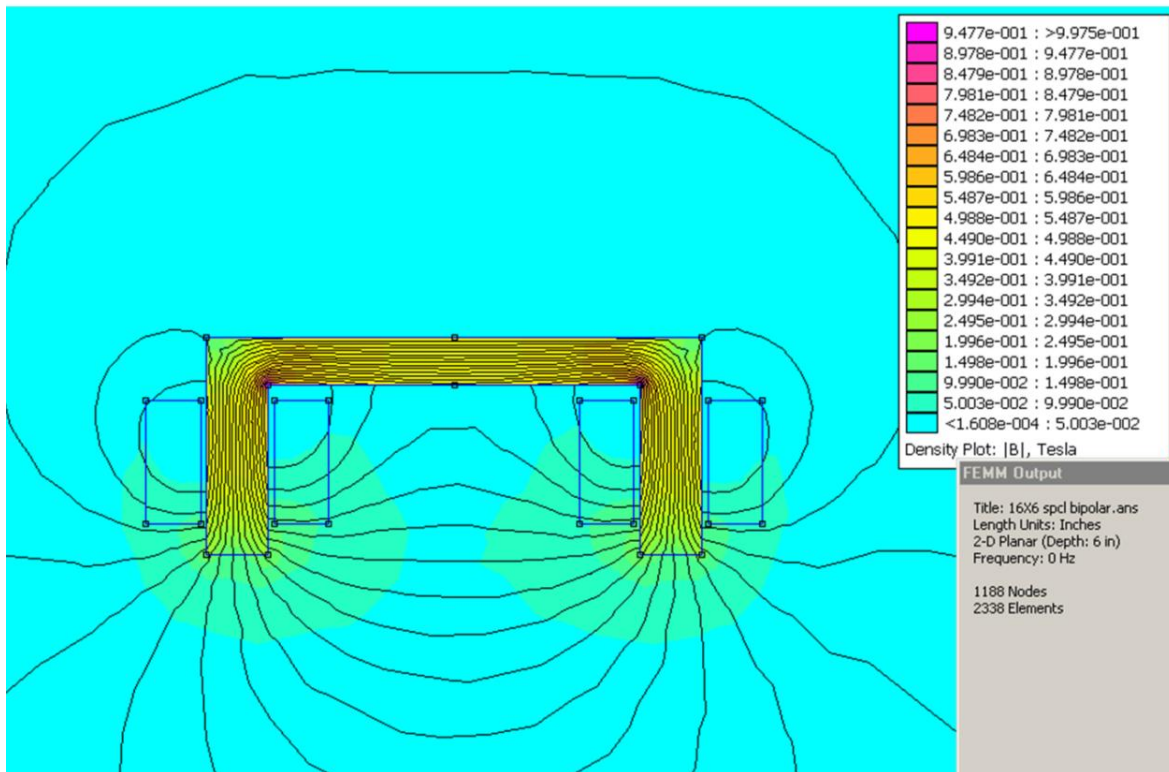


Figure 5: Simulation plot of magnetic flux density, $|B|$ [T], around the 16 in. x 6 in. bipolar electromagnet using FEMM.



Figure 6. The final prototype electromagnet-sensor designed and fabricated based on IMF method.

5.3 Sensors and Other Equipment

The electromagnet is one of the major components of the prototype sensor. The other components include the Hall sensors to measure the induced magnetic field and a data acquisition system (DAS) to record data from the sensors to a computer. For electrical protection of the electromagnet, an on-timer is used so that the magnet does not stay on past its safe duty cycle. A Lakeshore Gaussmeter is also used as a reliable backup for magnetic field measurements.

5.3.1 Hall Sensors

Hall sensors are mounted at various positions on the pole faces of the electromagnet to measure accurately the magnetic field at a particular point on the specimen. They measure the axial component of the induced magnetic field in the steel specimen. The sensor selected was Micro Switch Linear Output Hall Effect Transducer model SS94A2D. It has sensitivity of 1 mV/G and the magnetic flux measurement range is -2500 G to +2500 G. The characteristics of this sensor are linear in the region of operation at 25°C (see Figure 7). Sensors were mounted on the electromagnet pole face at a point of the highest magnetic field. Even though the sensors are rated for ± 2500 G, their characteristics hold true up to ± 4500 G. For some higher readings, the Gaussmeter was used as a backup.

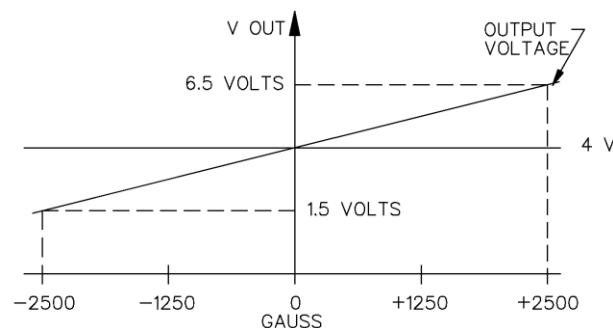


Figure 7: Characteristics of Hall sensor to be used sensing induced magnetic field (Micro Switch 2008).

5.3.2 Data Acquisition and Recording

An Optim MEGADAC data acquisition system was used to collect data from the sensors. This data is stored in the computer through an interface with the DAS. The Hall sensors are sourced through the DAS which measures the output voltage from the sensors and converts it to magnetic

field reading in terms of Gauss. This data can be recorded and made available for future reference. The DAS was initially calibrated and set at a sensitivity value to relate magnetic flux measurements to the output voltage. Figure 7 shows the setup used for the experiments using a prototype electromagnet-based sensor. Further description of experiments and details about the steel samples used are described in Section 6.

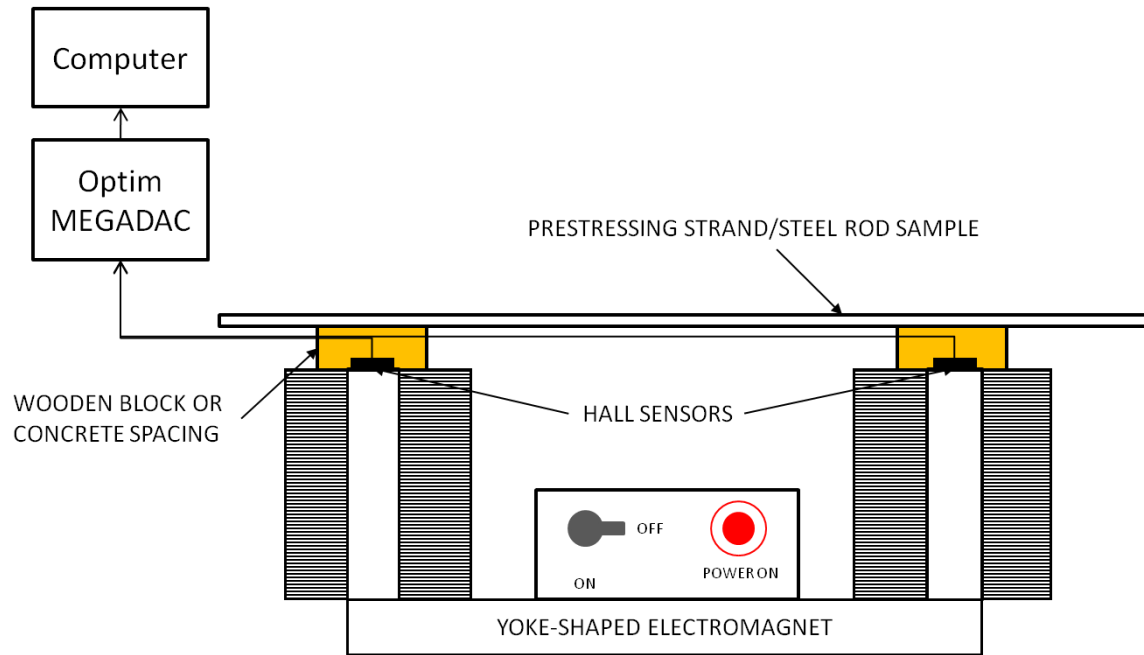


Figure 8: Setup of experiment using yoke-shaped electromagnet.

6. The Experiments with Yoke-Shaped Electromagnet Sensor

This section describes experiments conducted to test the effectiveness of the IMF method. The setup described in section 5 is used throughout to take measurements. Hollow wooden blocks were used to create air-gaps of different sizes, mounted on the pole faces. Concrete blocks of different sizes were used for experiments with concrete. The steel samples used were AISI 1018 steel and AISI 1020 7-wire prestressing strand of different sizes. Tests were performed using completely corroded strands obtained from a demolished bridge. Magnetic field measurements are used to estimate the loss of cross section. The measurements are tabulated and plotted later in Section 7 where the results are discussed in detail.

6.1 Experiments with AISI 1018 Cold-rolled Steel Bars

The general laboratory setup for magnetic field measurements of steel samples is shown in Figure 9. The first set of experiments was conducted using non-corroded AISI 1018 cold-rolled steel bars with circular cross section. The bars were of uniform diameters ranging from $\frac{1}{16}$ in. to $\frac{3}{4}$ in. This steel was chosen as it is closer in chemical composition to prestressing steel. Plain steel bars were used to check if the induced magnetic field stays uniform throughout the length of the bar. Table 1 shows the chemical composition of the two types of steel. Initially, air gaps

were used instead of concrete to see if results obtained are reliable enough to go on to the next step. The air-gaps are generated using hollow wooden blocks of different heights.

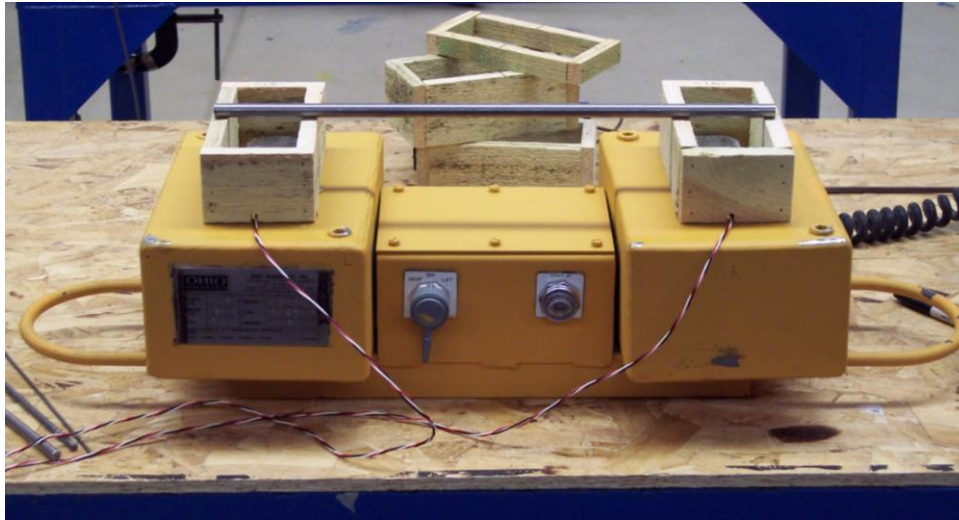


Figure 9. Experiment setup for magnetic field measurement of steel rod samples.

Table 1: Chemical composition of steels used.

Steel	Element (wt %)				
	C	Mn	P	S	Si
AISI 1018	0.17	0.77	0.012	0.03	0.19
Prestressing Strand (7-wire)	0.80-0.85	0.8-1.0	0.02	0.02	0.20-0.35

The steel specimen of length about 18 – 24 in. is placed over the wooden block and the electromagnet is turned on. As the magnetic field is induced in the specimen, the Hall sensors produce an output voltage which is available on the computer through the DAS. Two readings are available from the right and left pole sensors. Since these values are nearly close to each other, the right pole reading was recorded. Table 2 shows the induced magnetic field measurements recorded for different AISI 1018 steel rod sizes, each measured with different air gap sizes (0.125 in. to 2 in.). The different air gaps were chosen to simulate different sizes of depleting concrete cover in the bottom part of the bridge where the majority of the strands are located. The typical strand location for most bridges in Ohio is shown in Figure 10, both from the 1980s and the 2000s (ODOT 1981, 2002). It can be seen that the typical concrete thickness at the bottom of the box-girder is $1\frac{1}{4}$ in. or $1\frac{3}{4}$ in. It has also been seen that the maximum amount of corrosion occurs in the layer of strands closer to the base.

Table 2: Observations from experiments using air gap with AISI 1018 steel bars.

Steel rod dia. (in.)	Area (in ²)	Induced magnetic field (G) for different air-gap sizes								
		0.125 in.	0.25 in.	0.5 in.	0.75 in.	1 in.	1.25 in.	1.5 in.	1.75 in.	2 in.
1/8	0.0123	2090	1930	1633	1524	1485	1448	1423	1407	1387
3/16	0.0276	2700	2290	1773	1587	1524	1467	1439	1424	1395
1/4	0.0491	3200	2640	1900	1640	1560	1492	1460	1431	1408
5/16	0.0767	3550	2880	1990	1695	1595	1522	1483	1450	1420
3/8	0.1104	3970	3180	2100	1761	1644	1551	1510	1470	1435
7/16	0.1503	4280	3420	2230	1820	1700	1590	1543	1495	1455
1/2	0.1964	4680	3680	2360	1900	1753	1629	1572	1520	1473
9/16	0.2485	4960	3900	2490	1970	1800	1673	1608	1547	1493
5/8	0.3068	5400	4180	2600	2050	1870	1717	1640	1574	1513
11/16	0.3712	5740	4450	2760	2140	1930	1760	1683	1606	1536
3/4	0.4418	6070	4700	2900	2200	2000	1808	1723	1635	1555

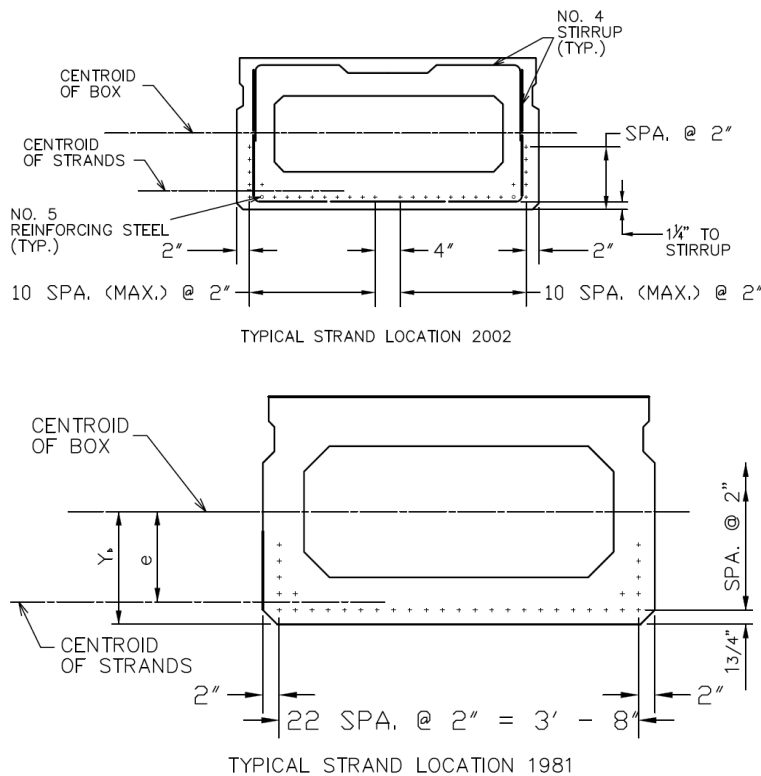


Figure 10: Strand locations in common box beam bridges in Ohio (ODOT 1981, 2002).

The next set of experiments is conducted using concrete blocks instead of air gaps. Blocks of different sizes cut from old blocks of concrete were used. Their sizes range from $7/8$ in. to $1^{15/16}$ in. thick. The block is mounted on top of the pole with a small gap ($1/8$ in.) in between to protect the sensors. Table 3 shows the readings taken for each steel rod measured with different concrete

blocks. Thus, twelve diameter sizes of AISI 1018 steel were used to measure their induced magnetic fields with air and concrete gaps of different sizes.

Table 3: Observations from experiments using concrete block with AISI 1018 steel bars.

Steel rod dia. (in.)	Area (in ²)	Induced magnetic field (G) for different concrete block sizes				
		0.75 in.	1 in.	1.1 in.	1.2 in.	1.8 in.
1/8	0.0123	1552	1492	1457	1433	1405
3/16	0.0276	1605	1518	1475	1454	1413
1/4	0.0491	1656	1544	1498	1470	1421
5/16	0.0767	1708	1572	1526	1497	1434
3/8	0.1104	1760	1608	1560	1525	1453
7/16	0.1503	1834	1648	1593	1563	1475
1/2	0.1963	1900	1694	1633	1597	1495
9/16	0.2485	1974	1742	1672	1638	1517
5/8	0.3068	2010	1787	1714	1675	1538
11/16	0.3712	2120	1830	1758	1728	1562
3/4	0.4418	2210	1880	1800	1771	1588

6.2 Experiments with Prestressing Strand

In this experiment, 7-wire prestressing strand samples of different diameters were used (See Figure 11). They were all in non-corroded and unstressed condition. Totally four sizes ranging from $\frac{3}{8}$ in. to $\frac{3}{5}$ in. diameter, were used. The same experiments as done for the AISI 1018 cold-rolled steel rebar were repeated with the prestressing strands. Readings from experiments with air gaps are shown in Table 4 and those done with concrete blocks are shown in Table 5. In this case too, the readings for the right pole were recorded since the strands are uniform all over.

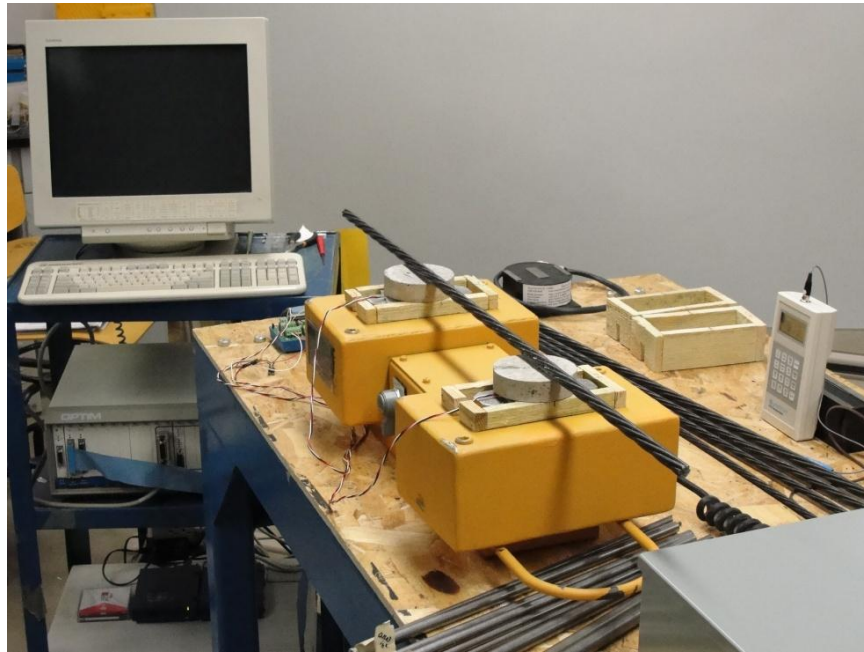


Figure 11: Experiment setup for magnetic field measurements of prestressing steel strand samples.

Table 4: Observations from experiments using air-gaps with non-corroded prestressing strands.

Strand Dia. (in.)	Area (in ²)	Induced magnetic field (G) for different air-gap sizes								
		0.125 in.	0.25 in.	0.5 in.	0.75 in.	1 in.	1.25 in.	1.5 in.	1.75 in.	2 in.
3/8	0.1104	3670	2850	2060	1740	1630	1530	1495	1453	1415
7/16	0.1503	4250	3290	2200	1830	1690	1580	1533	1478	1436
1/2	0.1963	4490	3560	2360	1940	1760	1620	1572	1512	1464
3/5	0.2827	5310	4070	2650	2090	1880	1711	1638	1566	1503

Table 5: Observations from experiments using concrete blocks with non-corroded prestressing strands.

Steel rod dia. (in.)	Area (in ²)	Induced magnetic field (G) for different concrete block sizes				
		0.75 in.	1 in.	1.1 in.	1.2 in.	1.8 in.
3/8	0.1104	1733	1595	1560	1540	1462
7/16	0.1503	1820	1645	1605	1590	1480
1/2	0.1963	1910	1700	1648	1637	1505
3/5	0.2827	2060	1790	1732	1712	1546

6.3 Experiments with Corroded Prestressing Strand

Corroded prestressing strand pieces obtained from a demolished bridge were used as test specimens to measure its average remaining cross sectional area using the IMF method. These strands had an original diameter of 0.5 in. and they were tested with 1 in. and 1.8125 in. thick concrete blocks. Measurements were taken at equidistant spots on the corroded strand along its length. Table 6 shows the magnetic field measurements for one such corroded strand. This test was done to predict the remaining cross sectional area of the corroded strands. The data from the non-corroded prestressing strands was used as a basis for these predictions.

Table 6: Observations from experiments using concrete blocks with corroded prestressing strands.

Length (in.)	Induced magnetic field (G) for corroded strand 0.5 in. thick	
	Concrete block 1 in. thick	Concrete block 1.8 in. thick
	2	1613
4	1678	1477
6	1693	1494
8	1679	1500
10	1674	1492
12	1659	1492
14	1644	1489
16	1629	1477
18	1600	1465
20	1575	1468
22	1590	1461
24	1603	1463
26	1606	1463

The results from all the experiments described in this section are analyzed and discussed in the Section 7.

7. Results and Data Interpretation

The final results with the new electromagnet have been encouraging. There is a consistent, easy to describe relationship between the remaining cross sectional area and concrete cover. Different steel sample diameters were used to obtain the induced magnetic field values in different cross sectional areas. Tables 7 and 8 show the different diameters of the AISI 1020 steel 7-wire prestressing and AISI 1018 steel samples with the corresponding percentage difference in cross sectional area for each sample used in the experiments. It is seen that the average change in the cross sectional area is about 36% for prestressing strand and change ranges from around 20% up to above 100% for AISI 1018 steel rods. Tests were conducted using both air gaps and concrete for all the samples to study the magnetic reluctance of concrete.

Table 7: Sizes of AISI 1020 steel 7-wire prestressing strand used in the experiments.

Diameter [in.]	Effective cross sectional area (A) [in ²]	% Change in cross section
0.375	0.1104	0
0.4375	0.1503	36.11
0.5	0.1963	30.61
0.6	0.2827	44

Table 8: Sizes of AISI 1018 steel strand used in the experiments.

Diameter [in.]	Cross sectional area (A) [in ²]	% Change in cross section
0.125	0.0123	0
0.1875	0.0276	125.00
0.25	0.0491	77.78
0.3125	0.0767	56.25
0.375	0.1104	44.00
0.4375	0.1503	36.11
0.5	0.1963	30.61
0.5625	0.2485	26.56
0.625	0.3068	23.46
0.6875	0.3712	21.00
0.75	0.4418	19.01

7.1 Comparison of Steel Samples Magnetized in Air Gaps

IMF measurements for the steel samples of AISI 1018 cold rolled steel rods and AISI 1020 prestressing steel strands, using air gaps of different sizes in steps from 0.75 in. up to 2 in. are plotted in Figure 12 (using Tables 2 and 4). From the graphs it can be seen that the induced magnetic field is proportional to the corresponding cross sectional area of the steel sample. This is true for both types of steel samples used. It can also be seen that the prestressing steel is comparatively magnetized to a higher extent than the AISI 1018 steel rods. This can be attributed to the higher carbon content in prestressing steel. Thus, the metallurgy has an effect on the amount of magnetic field induced in the steel sample. A complicating factor in the field scenario would be presence of any ferromagnetic material such as transverse shear reinforcement in addition to the strand in a prestressed concrete beam.

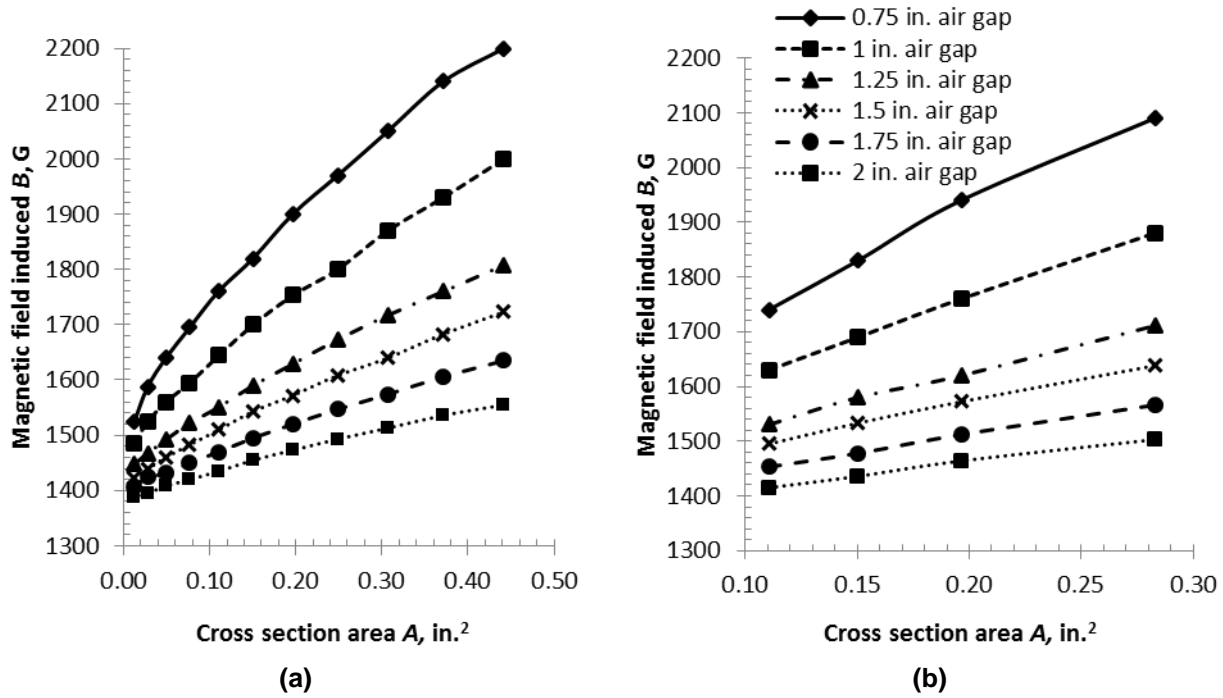


Figure 12: Induced magnetic field, (B) [G], for samples of cross sectional area, (A) [in^2], for different air-gaps (a) AISI 1018 steel rods, (b) 7-wire prestressing steel strands.

7.2 Comparison of Steel Samples Magnetized in Concrete Blocks

The results from IMF measurements for both types of steel samples using concrete gaps is plotted in Figure 13 (using Tables 3 and 5). By comparing Figures 12 and 13 it can be seen that concrete has a slight damping effect on the magnetization for both types of steel. From both these figures it is clear that the magnetic field induced in the steel sample can give a measure of the corresponding cross sectional area of the sample. This appears true for all the air gaps and different concrete block sizes used for the experiment. In the case of concrete blocks it can be seen that prestressing strand has a comparatively higher amount of induced magnetic flux. Thus, concrete has a positive effect on magnetization of prestressing strand.

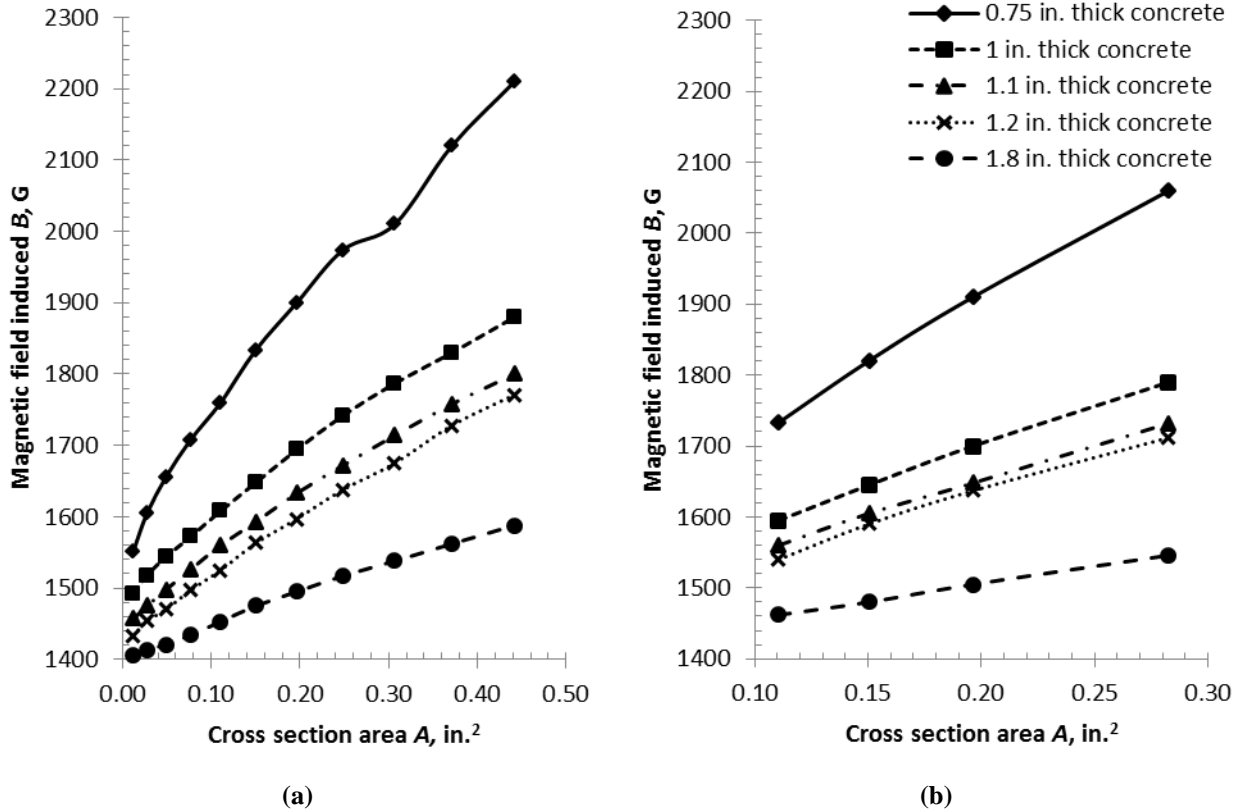


Figure 13: Induced magnetic field, (B) [G], for samples of varying cross sectional area, (A) [in.^2], for different concrete blocks (a) AISI 1018 steel rods, (b) 7-wire prestressing steel strands.

7.3 Analysis for Corroded Prestressing Strand

Corroded prestressing strand pieces from a demolished bridge were used as test specimens to estimate the average remaining effective cross sectional area. The original diameter of the strands was 0.5 in. They were magnetized using 1 in. and 1.8 in. thick concrete blocks. Figure 14 shows induced magnetic field measurements for one such corroded strand along a section of its length (using Table 6). The variation in the measured magnetic field indicates corresponding loss of volume and decrease in cross sectional area.

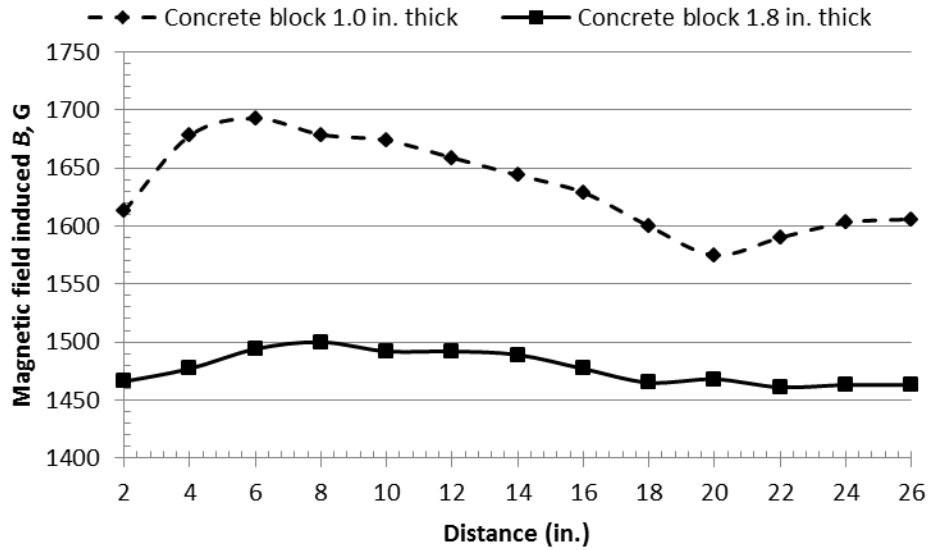


Figure 14. Magnetic field measurements for a corroded prestressing strand along a section of its length with two types of concrete blocks – 1 in. thick and 1.8 in. thick.

The next step was to use the induced magnetic field values from Figure 13(b), obtained previously in the laboratory for non-corroded prestressing strands, to estimate the remaining effective cross sectional area of the corroded strands. The induced magnetic field measured by the Hall sensor on the pole face is directly related to the effective cross sectional area of the magnetized strand. By knowing the effective cross sectional area at different points along the length of the strand, the remaining strength of the steel strand can be estimated. Figure 14 shows cross sectional area estimations made for the corroded strand section using the curves of induced magnetic field for concrete blocks – 1 in. and 1.8 in. thick, from Figure 13(b). It is necessary to know the concrete cover depth in order to use the right curve to estimate effective cross sectional area. The two curves in Figure 15 show the variation in effective remaining cross sectional area along the section of the corroded strand. A comparison of the estimated cross sectional area to the actual effective cross sectional area is a way to assess the accuracy of the proposed magnetic field approach. To do this the strand was cut at different points along its length and the remaining effective cross sectional area was measured. The comparison of the measured and estimated values of cross sectional area is shown in Table 9.

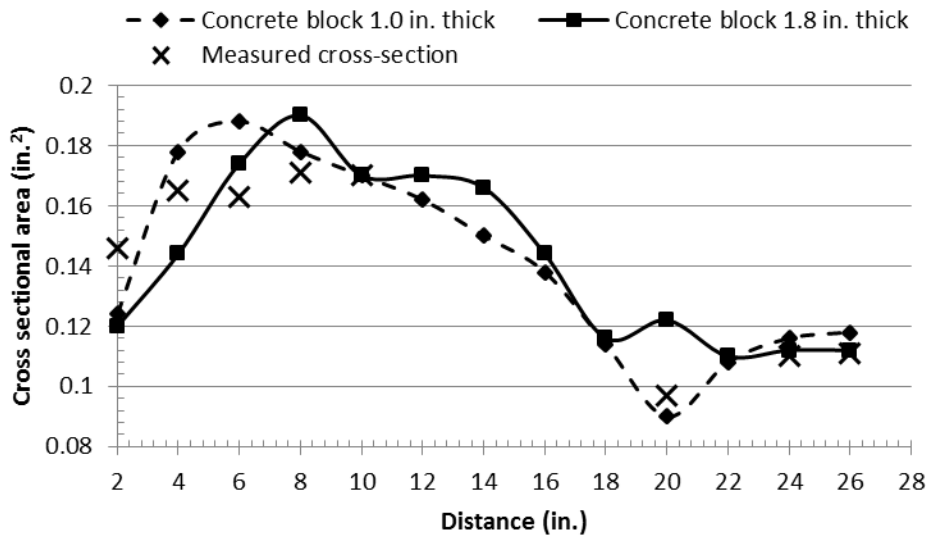


Figure 15. Effective remaining cross sectional area estimated for the corroded prestressing strand specimen, from induced magnetic field values.

Table 9. Corroded prestressing sample strand estimated effective remaining cross section from Figure 15.

Length [in.]	Concrete block 1 in. thick [in.²]	Concrete block 1.8 in. thick [in.²]	Measured cross sectional area [in.²]	Maximum deviation [in.²]
2	0.124	0.12	0.146	0.026
4	0.178	0.144	0.165	0.021
6	0.188	0.174	0.163	0.025
8	0.178	0.19	0.171	0.019
10	0.170	0.17	0.170	0.000
12	0.162	0.17	n.d.	n.d.
14	0.150	0.166	n.d.	n.d.
16	0.138	0.144	n.d.	n.d.
18	0.114	0.116	n.d.	n.d.
20	0.090	0.122	0.097	0.025
22	0.108	0.11	n.d.	n.d.
24	0.116	0.112	0.110	0.006
26	0.118	0.112	0.111	0.007

Note: n.d. – no data. Some values could not be measured due to subsequent crumbling of the strand during measurements.

At each point along the section length, two cross sectional area values are estimated - one for magnetization with 1 in. thick concrete block and the other for 1.8 in. thick block. *e.g.* at the length of 8 in. on the strand, the estimated effective remaining cross sectional area with 1 in. thick concrete block is 0.178 in.² and with 1.8 in. thick concrete block is 0.19 in.². The measured cross sectional area value for that point is 0.171 in.². It can be observed that the maximum difference of the estimated values from the measured value at this point is 0.019 in.². From all the values predicted in the Table 9, it can be seen that the maximum difference between estimated and measured values is 0.026 in.².

From all these experiments, it can be seen that the IMF technique successfully shows the difference in diameters (or cross section) for AISI 1020 steel prestressing strand and AISI 1018 steel rods. Thus, this magnet-sensor prototype can be used with good accuracy to predict the loss of section due to corrosion from the changes in magnetic properties of prestressing strand. Further improvements in sensitivity of the detection mechanism would allow researchers to use this detection system on a bridge by incorporating additional features like a detection mechanism for locating the strands inside the concrete for proper magnetization.

The next step in validating this prototype sensor was to use it on a bridge to detect corrosion. This and other concerns have been described in section 8.

8. Overview of Development of the IMF Sensor System

A magnetic sensor system to detect the remaining cross sectional area of prestressing strand in concrete beams was designed and tested in the laboratory. A magnetic approach has inherent advantages as it directly detects the remaining area, it measures the whole volume of the material and it detects flaws that are not visible from surface inspection. The laboratory results have shown potential for the sensor system to evaluate a bridge in the field to prove its reliability. The electromagnet-sensor system proved to be successful in the field. Work to make it practical is required, after which it can be widely applied by bridge inspection engineers to evaluate such infrastructure and carry out maintenance measures on time to save the life of the bridge by preventing further deterioration.

8.1 Field Test on Washington Waterloo Road Bridge

To validate the prototype sensor system a nondestructive testing of a box beam bridge to evaluate the condition of the prestressing strand was carried out. A bridge on Washington Waterloo Road in Ohio (see Figure 16) which was scheduled for demolition by ODOT (ODOT 2008) was identified for the purpose. Permission was obtained in 2010 (as part of a sub-contract with ODOT through Ohio University) to conduct a series of tests designed to take advantage of the characteristics of the bridge. Field measurements were taken before demolition using the IMF technique and then after it was demolished the strand was dissected and visually assessed for its effective cross sectional area. In addition to the IMF method, an MFL system developed by Dr. Al Ghorbanpoor was used to evaluate the condition of the box beams. The MFL system developed by him has been successful in determining fractures in prestressing strand (Ghorbanpoor *et al.* 2000) and quantifying corrosion in strands from the characteristics of the magnetic flux leakage signal obtained. These findings will be available through ODOT after publication of the final report (Nims and Devabhaktuni 2011). It was found that there was a close match between the estimations of the IMF, MFL and visual inspection methods. Some issues causing reduction in accuracy of cross section estimations were identified; they have been discussed in detail in that report.

It is crucial to know the distance between the strand and the Hall sensor on the pole face of the electromagnet accurately, in order to have a good estimation of the remaining cross sectional area of the strand. It becomes difficult to measure this distance accurately sometimes due to a curvature in the bridge. The strand inside the box beam might also not always be horizontal. Work is in progress to use a magnetic method to determine the strand depth accurately. Other

issues are mostly related to physical aspects of the system. When the sensor system is turned on for a considerable amount of time there is a drift in the measured values due to temperature rise caused by self-heating. This can be brought under control by using a temperature sensor and determining the stable operating temperature range of the sensor system. Its heavy weight is of concern since it prevents smooth motion of the electromagnet-sensor while performing a scan under the bridge. It also causes inconvenience for easy handling during testing. A good support system needs to be used, which can be suspended from under the bridge (possibly by using weep holes in the box beams). This support system should enable the sensor to move along the length of the box beam in a controlled manner to magnetize the strands and take measurements.



Figure 16: Washington Waterloo road bridge, Ohio.

8.2 Present State-of-the-Art and Progress

At present the IMF sensor system has been tested and evaluated in the laboratory. It has also been tested in the field over a bridge by comparing with MFL and visual inspection methods. The results have been good and provide a proof-of-concept for the IMF method. Issues that need to be dealt with have been identified. To scan multiple strands being magnetized, an array of Hall sensors on the pole face is used to record induced magnetic field in each strand. For this it is necessary to locate the strands as closely as possible.

Magnetic inspection techniques have been demonstrated in the laboratory and used in the field. IMF, RMF, and MFL have different strengths and weaknesses. The IMF method gives a direct measure of the remaining effective cross section area of a prestressing strand. However, it requires stronger magnetization (which requires a heavier electromagnet) and accurate knowledge of the distance between the strand and the electromagnet. The MFL and RMF method detects fractures in prestressing strands and quantifies the condition of the strand in terms of the percentage of corrosion, both having close accuracy (Jones *et al.* 2010). However, it would be more advantageous to have a method which detects early corrosion and gives a direct measure of the cross section area, which is helpful in load rating of the bridge. However, the trade-offs need to be carefully considered before selecting a technique for widespread implementation. Overall, to advance the art of magnetic inspection the following tasks need to be done:

1. Carry out the inspection and dissection of box beams that have been removed from service with corroded strands to increase the database for the correspondence between magnetic signals and strand condition.
2. Develop guidelines for systematic visual assessment to prioritize magnetic inspection of a bridge inventory and reduce the area on each bridge that needs to be scanned. Crack patterns on the soffit can indicate corrosion in the strand. Make inspection more efficient by limiting the area that is inspected. Too much detail in inspection is costly and does not result in a significant improvement in the load rating; too little information leads to inaccurate load rating.
3. Incorporate magnetic inspection into bridge load rating. This allows the convenient use of magnetic inspection data by owners in a format they are familiar with. In the long term, it would be desirable to use magnetic inspection data in reliability models.
4. Computation Prediction Model: A prediction model would be useful in determining the effective remaining cross section from the measured magnetic field values. A computer simulation model of the electromagnet-sensor based on the magnetic field equations to predict the magnetic field induced in the prestressing strand depending on its cross section and depth embedded in the concrete has also been developed. Such a model can be used to compare measured field values with simulated induced magnetic field values to estimate the cross sectional area of the prestressing strand. In this model, parameters such as permeability of the steel used for the prestressing strand, thickness of the concrete cover, distance between adjacent strands inside a concrete beam, *etc.*, are taken into consideration.
5. Both IMF and MFL methods produce a signal which is visually interpreted. Software to apply signal analysis tools to extract information from the measured signal regarding the condition of the strand embedded inside the box beam needs to be developed.
6. Design a better support system to scan the smooth soffit of box beam bridges. A semi-automated mechanical system that can maneuver the sensor unit under the bridge is desirable. Review existing mechanical systems to determine if any are suitable for the deployment of the magnetic sensor on the underside of box beam bridges.
 - Develop a prototype improved support system.
 - Carry out proof of concept testing of the support system.
7. Enhance the magnetic signature of strand. There are chemical additives which can enhance the magnetic signature of corrosion. The potential of treating strand and concrete to enhance future inspection should be investigated.

9. Conclusions and Future Work

This section gives an account of the conclusions derived from all the work conducted in Phase II of this project including field tests. Future work necessary to bring about practical implementation of the magnetic sensor system is mentioned.

9.1 Conclusion

A proof-of-concept of the IMF method proposed as a tool for nondestructive testing of prestressed box beams has been presented. The following goals were achieved:

1. An electromagnet-sensor system was designed and fabricated after conducting preliminary experiments using an industrial lifting electromagnet. The induced magnetic field in steel rod specimens was correlating to the cross section (or diameter) of the steel sample. The same was also verified for different diameter sizes. Laboratory experiments were done with non-corroded steel rods and prestressing strands.
2. Corroded prestressing strands were examined and their remaining cross sectional area was estimated with good accuracy. Thus, laboratory experiments using the prototype electromagnet-sensor have shown that the magnetic method has potential to estimate the remaining effective cross sectional area of prestressing strands. Overall, it was observed that laboratory results could demarcate the difference in specimen diameters (and effective cross section) from the levels of the induced magnetic field.
3. External funding was sought to perform field tests using the prototype sensor. Field tests have been conducted as part of this other project to determine efficacy of the IMF method. These tests have also shown that the magnetic method has ability to locate corrosion in prestressing strands. Further refinement is, however, necessary to improve its estimation accuracy. To fabricate the system the team was successful in developing a partnership with Ohio Magnetics who could understand the problem being addressed and thus, were able to provide a reasonable design for the research magnet.

In the development of this sensor, the primary challenges are the difficulty of magnetizing the specimen from one side and knowing the distance accurately between the strand and the electromagnet-sensor pole face. Other concerns are the weight of the electromagnet and drift in measured values due to self-heating. This, however, is mitigated by laboratory results and field tests that show a close match with measured cross sectional area values. With these issues sorted out and by using a computer simulated prediction model characterized on the electromagnet-sensor, practical implementation of this testing system should not be far off. Such a practical sensor, once developed, should be able to estimate the area of exposed or hidden corroded strands. The development of a magnetic sensor will make inspection of prestressed concrete bridges easier and more cost effective by assisting in effective maintenance planning.

9.2 Future work

The present work and that of others has shown magnetic techniques are a theoretically viable technology. Box girders are practical and economical. The steps that need to be taken to advance this work have been identified.

References

- American Association of State Highway and Transportation Officials (AASHTO) (2011), “The Manual for Bridge Evaluation,” second edition, Washington, DC.
- Abi Shdid (2006), C. and M.H. Ansley “Visual Rating and Strength Testing of 40-Year-Old Precast Prestressed Concrete Bridge Piling”, *Transportation Research Record: Journal of the Transportation Research Board No. 1975*, July 2006.
- Naito (2010), C. and L. Jones, “Nondestructive Inspection of Strand Corrosion in Prestressed Concrete Box Beam Members,” *NDE/NDT for Highways and Bridges: Structural Materials Technology Conference*, New York City.
- Federal Highway Administration (FHWA 2010), “Inspection Methods and Techniques to Determine Non-visible Corrosion of Prestressing Strands in Concrete Bridge Components” TPF-5(167), <http://www.pooledfund.org/projectdetails.asp?id=393&status=6>, accessed April 30, 2010.
- Ferroni (2007), K., “Inspection Methods and Techniques to Determine Non-visible Corrosion of Prestressing Strands in Concrete Bridge Components” <http://rip.trb.org/browse/dproject.asp?n=15188>, accessed Nov. 16, 2008.
- Ghorbanpoor (2000), A. R. Borchelt, M. Edwards and E. Abdel Salam, “Magnetic-Based NDE of Prestressed and Post-Tensioned Concrete Members – The MFL System,” Final Report FHWA-RD-00-026, Federal Highway Administration, US Department of Transportation, McLean, VA.
- Hillemeir (1998), B. and H. Scheel, “Magnetic detection of prestressing steel fractures in prestressed concrete”, *Materials and Corrosion*, Vol. 49, pp 799-804.
- Jones (2010) L., S. Pessiki, C. Naito, and I. Hodgson, Inspection methods & techniques to determine non visible corrosion of prestressing strands in concrete bridge components, Task 2 – Assessment of candidate NDT methods. Lehigh University, ATLSS Report No. 09-09.
- Kusenberger (1981), F.N., and J.R. Barton, “Detection of Flaws in Reinforcement Steels in Prestressed Concrete Bridges” Final Report FH-WA/RD-81/087, Federal Highway Administration (FHWA), Washington, DC.
- Micro Switch (2008), “Linear output Hall effect transducer SS94A2D,” datasheet rev. E, page 1 of 1.
- Nims (2011), D. and Devabhaktuni, V., “Magnetic Inspection of the Prestressing Strand of the Washington-Waterloo Rd, Fayette Co., Ohio,” report submitted to Ohio University for Ohio Department of Transportation.

- Ohio Department of Transportation (ODOT) (December 1981). Design Data for Prestressed Concrete Bridge 24 ft. Roadway Width Non-Composite 48" Adjacent Box Beams with Straight Strands. pp. 1.
- Ohio Department of Transportation (ODOT) (October 2002). Design Data: Prestressed Concrete Non-Composite Adjacent Box Beams (48" Wide) with Straight Strands. Drawing PSBDD-2-07. pp. 1.
- ODOT (2008) Ohio Department of Transportation Request for Proposals "Structural Evaluation of LIC-310-0396 Box Beams with Advanced Strand Deterioration, PS-08-11.
- Rumiche (2008), F., Indacochea and M.L. Wang, "Detection and Monitoring of Corrosion in Structural Carbon Steels Using Electromagnetic Sensors", *Journal of Engineering Materials and Technology*, ASME, Vol. 130.
- Russell, H.G., "Adjacent precast concrete box-beam bridges: State of the practice" *PCI Journal*, pp. 75-91, Winter 2011.
- Sawade (2007), G. and H-J. Krause. Inspection of Prestressed Concrete Members Using the Magnetic Leakage Flux Measurement Method – Estimation of Detection Limit. *Advances in Construction Materials*, pp. 639-649.
- Scheel (1997), H.: *Spannstahlbruchortung an Spannbetonbauteilen mit nachtraglichem Verbund unter Ausnutzung des Remanenzmagnetismus*, Dissertation, Technical University, Berlin.
- Scheel, H. and Hillemeier (1997), B., "Capacity of the remnant magnetism method to detect fractures of steel in tendons embedded in prestressed concrete", *NDT & E International*, Vol. 30, No. 4, pp 211-216.
- Scott (2006), C.M., PA Non-composite Adjacent Box Beam Bridges A presentation adapted from the AASHTO T-18 Bridge Inspection Technical Committee Meeting, June 2006.

Appendix

Bipolar Electromagnet 16 in. x 6 in. Drawing

